The Plant Cell, Vol. 27: 3354–3366, December 2015, www.plantcell.org

MicroRNA miR396 Regulates the Switch between Stem Cells and Transit-Amplifying Cells in Arabidopsis Roots

Ramiro E. Rodriguez,[a,1] María Florencia Ercoli,[a] Juan Manuel Debernardi,[a] Natalie W. Breakfield,[b] Martin A. Mecchia,[a] Martin Sabatini,[a] Toon Cools,[c,d] Lieven De Veylder,[c,d] Philip N. Benfey,[b] and Javier F. Palatnik[a,1]

[a] Instituto de Biología Molecular y Celular de Rosario, CONICET, Facultad de Ciencias Bioquímicas y Farmacéuticas, Universidad Nacional de Rosario, 2000 Rosario, Argentina

[b] Department of Biology and Howard Hughes Medical Institute, Duke University, Durham, North Carolina 27708

[c] Department of Plant Systems Biology, VIB, 9052 Ghent, Belgium

[d] Department of Plant Biotechnology and Bioinformatics, Ghent University, B-9052 Ghent, Belgium

ORCID IDs: 0000-0002-0867-4099 (R.E.R.); 0000-0001-5587-6227 (M.F.E.); 0000-0002-4591-7061 (J.M.D.); 0000-0001-8517-885X (N.W.B.); 0000-0001-9560-017X (M.S.); 0000-0002-1258-5531 (T.C.); 0000-0001-7996-5224 (J.F.P.)

To ensure an adequate organ mass, the daughters of stem cells progress through a transit-amplifying phase displaying rapid cell division cycles before differentiating. Here, we show that *Arabidopsis thaliana* microRNA miR396 regulates the transition of root stem cells into transit-amplifying cells by interacting with *GROWTH-REGULATING FACTORs* (*GRFs*). The *GRFs* are expressed in transit-amplifying cells but are excluded from the stem cells through inhibition by miR396. Inactivation of the *GRFs* increases the meristem size and induces periclinal formative divisions in transit-amplifying cells. The GRFs repress *PLETHORA* (*PLT*) genes, regulating their spatial expression gradient. Conversely, PLT activates *MIR396* in the stem cells to repress the *GRFs*. We identified a pathway regulated by GRF transcription factors that represses stem cell-promoting genes in actively proliferating cells, which is essential for the progression of the cell cycle and the orientation of the cell division plane. If unchecked, the expression of the *GRFs* in the stem cell niche suppresses formative cell divisions and distorts the organization of the quiescent center. We propose that the interactions identified here between miR396 and *GRF* and *PLT* transcription factors are necessary to establish the boundary between the stem cell niche and the transit-amplifying region.

INTRODUCTION

Both plants and animals rely on stem cells for the generation of the different cell types that constitute their body parts. Stem cells are located within specific cellular contexts referred to as stem cell niches (SCNs). As stem cells divide slowly, their progeny generally undergo rapid, transient amplifying cell divisions to ensure that there are enough cells for proper organ growth before differentiation. Cells undergoing this process are called transit-amplifying cells (TACs) (Koster and Roop, 2007; Scheres, 2007; Lui et al., 2011; Heidstra and Sabatini, 2014).

In plants, the root SCN is formed by the quiescent center (QC) and the adjacent stem cell initials (Petricka et al., 2012), which are specified by two parallel pathways: the PLETHORA (PLT) and SHORTROOT (SHR)/SCARECROW (SCR) pathways (Petricka et al., 2012; Heyman et al., 2014).

SHR and *SCR* encode members of the GRAS family of transcription factors (named after the first three members, GIBBERELLIC-ACID INSENSITIVE, REPRESSOR of GAI, and SCR) (Pysh et al., 1999). *SHR* expressed in the stele moves into the QC and cortex/endodermal initials (Nakajima et al., 2001) to activate *SCR* expression (Levesque et al., 2006). In turn, SCR maintains QC and stem cell identity (Sabatini et al., 2003), in part by inducing the expression of *WUSCHEL-RELATED HOMEOBOX5*, a QC-specific gene (Sarkar et al., 2007).

PLT proteins are expressed in a gradient along the longitudinal axis of the root that is established by a combination of cell-to-cell movement and mitotic segregation of proteins from a narrow transcriptional domain located in the stem cell region (Galinha et al., 2007; Mähönen et al., 2014). The highest level of PLT protein is found in the stem cell area, where it specifies stem cell identity (Aida et al., 2004; Galinha et al., 2007; Mähönen et al., 2014). The progeny of the proximal stem cells express a lower level of PLT and undergo new rounds of rapid cell divisions before they start to elongate and differentiate (Galinha et al., 2007; Mähönen et al., 2014). TACs require the expression of *PLT* genes, albeit to lower levels than in the stem cells (Galinha et al., 2007; Mähönen et al., 2014).

Small RNAs are crucial regulators of gene expression in animals and plants and play a major role in development (Bologna and Voinnet, 2014). One class of small RNAs, the 21-nucleotide microRNAs (miRNAs), is defined by their biogenesis pathway, which requires the cleavage of a fold-back precursor RNA by a ribonuclease type III called DICERLIKE1 (Bologna and Voinnet, 2014). The miRNAs inhibit gene expression by forming a complex containing an ARGONAUTE (AGO) protein, generally AGO1 (Mallory et al., 2008), and then guiding the complex to specific target RNAs that are complementary to the miRNA. This represses

[1] Address correspondence to rrodriguez@ibr-conicet.gov.ar or palatnik@ibr-conicet.gov.ar.

The authors responsible for distribution of materials integral to the findings presented in this article in accordance with the policy described in the Instructions for Authors (www.plantcell.org) are: Ramiro E. Rodriguez (rrodriguez@ibr-conicet.gov.ar) or Javier F. Palatnik (palatnik@ibr-conicet.gov.ar).

www.plantcell.org/cgi/doi/10.1105/tpc.15.00452

the translation of the target RNAs or promotes their degradation, inhibiting production of the encoded protein.

The genome of *Arabidopsis thaliana* contains more than 200 miRNA genes grouped into families according to sequence similarity. The miR396 family is encoded by two genes, *MIR396A* and *MIR396B*, and regulates the expression of transcription factors belonging to the *GROWTH-REGULATING FACTOR* (*GRF*) class (Rodriguez et al., 2010; Debernardi et al., 2012). The *GRF* transcription factors are defined by the presence of the WRC and QLQ protein domains involved in DNA binding and protein-protein interactions, respectively (Kim et al., 2003). There are nine *GRFs* encoded in the Arabidopsis genome, and seven of them have a target site for miR396 (Jones-Rhoades and Bartel, 2004). The miR396-GRF interaction is conserved among angiosperms and gymnosperms (Jones-Rhoades and Bartel, 2004; Debernardi et al., 2012). It has been shown that overexpression of miR396 represses organ growth in Arabidopsis (Liu et al., 2009; Rodriguez et al., 2010; Bao et al., 2014; Liang et al., 2014b), whereas increased levels of the *GRFs* promote growth, especially in leaves (Kim et al., 2003; Horiguchi et al., 2005; Rodriguez et al., 2010), yet the mechanisms underlying the functions of the GRFs are largely unknown.

Here, we show that the miR396/GRF regulatory network regulates the transition of stem cells to transit-amplifying cells in the root meristem. *GRFs* are expressed in TACs, while miR396 is expressed in the SCN. The GRFs are essential for the function of the TACs: downregulation of their expression resulted in a decrease in the rate of the cell cycle and generated periclinal cell divisions typical of stem cells among the TACs. By contrast, the activity of miR396 is necessary to exclude the GRFs from the SCN. If unchecked, the GRFs induce the formation of distorted QC and columella cells. Corresponding with the phenotypic observations, high miR396 levels activate in the TACs the expression of *PLT* genes and other marker genes that are normally expressed in the SCN. In turn, PLT activity is required for the expression of *MIR396* genes inside the SCN. Therefore, the interactions between miR396, *GRF*, and *PLT* initiates the transition between stem cells and the TACs.

RESULTS

miR396 Helps Determine the Architecture of the Root Meristem

Several *GRF* transcription factors are highly expressed in the meristematic region of the root (Supplemental Figure 1A), as determined using publicly available transcriptome data sets (Brady et al., 2007). We analyzed the expression pattern in more detail for two of these *GRFs*, *GRF2* and *GRF3*, which are also regulated by miR396 (Figure 1A). To do this, we prepared translational reporters for GRF2 and GRF3, which consist of either GRF2 or GRF3 fused to GFP (*GRF2-GFP* and *GRF3-GFP*). Both GRF2 and GRF3 were detected in the meristematic zone (Figures 1B and 1C), and more specifically in TACs, consistent with a role of the GRFs in the promotion of cell proliferation.

We then examined the triple mutant *grf1 grf2 grf3* and found the meristematic zone to be larger in size compared with the wild type (Figures 1D and 1H). Previous results have shown that a decrease of *GRF* levels due to the overexpression of miR396 causes a reduction in the number of cells and the size of the shoot apical meristem (Kim and Lee, 2006; Rodriguez et al., 2010). Therefore, although the increase in the root meristem size of *grf1 grf2 grf3* was moderate, the result was unexpected, considering the previous data obtained using the aerial part of the plant.

We generated a series of miR396 overexpressors to simultaneously downregulate all miR396-regulated *GRFs* (Figure 1E). We found that overall root growth was diminished in most of the transgenic plants expressing miR396 under the control of the strong 35S promoter (36 out of 50 primary transgenic plants) (Figure 1E; Supplemental Figure 2B). Cellular analysis of the line *35S:miR396* #2, which overexpresses moderate levels of miRNA *MIR396b*, showed that it had a larger meristematic zone due to an increase in both meristematic cell area and number (Figures 1F, 1I, and 1J). This is in agreement with the phenotype of *grf1 grf2 grf3* and confirms that the miR396:GRF ratio has different effects in the root and shoot apical meristems. We used RT-qPCR to measure the expression of the *GRFs* in this transgenic line and in mutants and observed a significant reduction in the transcript levels of six of the *GRF* transcription factors (Supplemental Figure 2A). This may explain the stronger effects observed in this line compared with *grf1 grf2 grf3* (Figures 1D and 1H). In addition, RT-qPCR analysis of the *GRFs* revealed that some of them were induced in this triple mutant (Supplemental Figure 1B), which might partially compensate for the loss of *GRF1*, *GRF2*, and *GRF3*.

Transgenic plants expressing the highest amounts of miR396, (*35S:miR396* #1) had an even larger meristematic zone (Figure 1F). However, these plants also displayed other root defects, such as a reduced elongation zone (Figure 1F) and short mature cells (Supplemental Figure 2C). We conclude that the balance between miR396 and the *GRFs* has a primary effect on meristem size, whereas strong accumulation of miR396 severely affects the overall longitudinal patterning of the root.

To assess the importance of the miR396/*GRF* balance in the root meristem, we used an artificial miRNA that targets *GRFs* with higher efficiency than does miR396 by removing a bulged nucleotide between positions 7 and 8 of the binding site (Figure 1A) (Debernardi et al., 2012). Plants expressing this artificial miRNA also had an enlarged root meristem (Figure 1G) and exhibited stronger effects on root growth (Supplemental Figure 3) than miR396 overexpressors, consistent with the enhanced interaction with the *GRFs*.

Disruption of miR396 Function Reduces Root Meristem Size

As insertional knockouts in *MIRNA* precursors are difficult to obtain due to their small size, we turned to target mimicry technology, which is based on the expression of a noncoding RNA that sequesters the miRNA (Franco-Zorrilla et al., 2007; Todesco et al., 2010). We analyzed plants expressing a mimic directed against miR396 (*MIM396*) containing three miRNA binding sites designed as sponges for miR396 (Figure 2A). Analysis by laser scanning confocal microscopy of the root tip cellular architecture revealed that the decreased miR396 levels found in *MIM396* plants (Supplemental Figure 4A) caused a moderate reduction in the size of the meristem (Figure 2B; Supplemental Figure 4B).

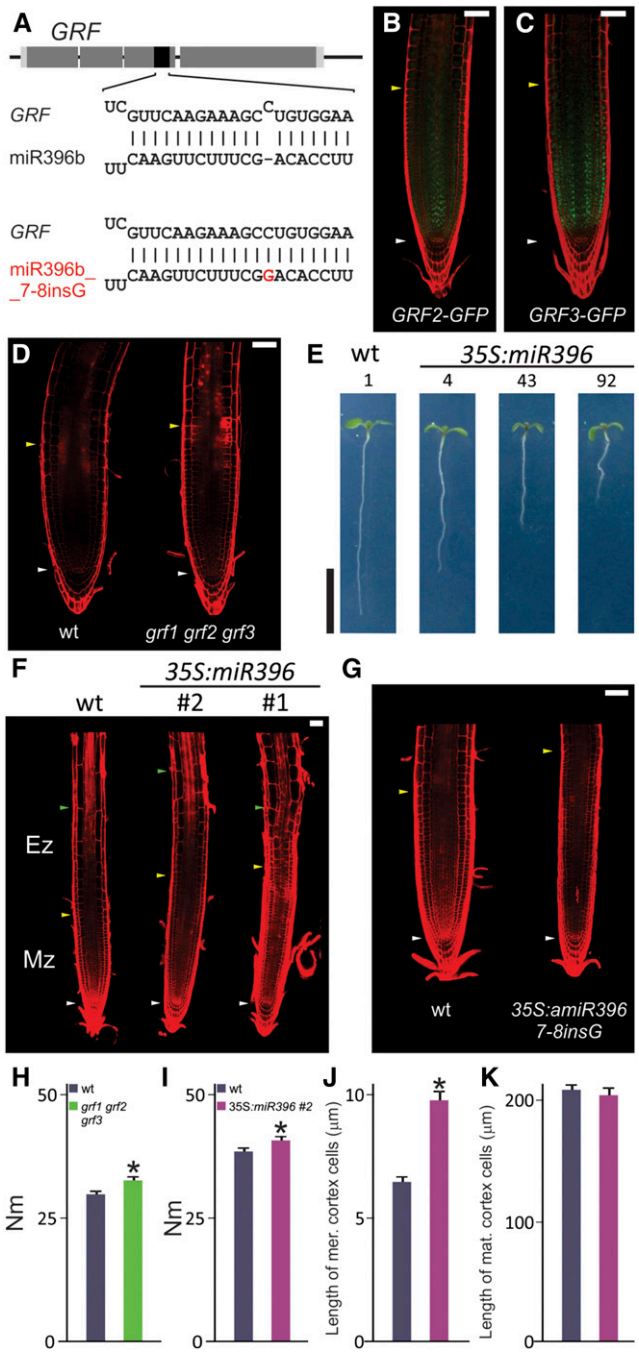

Figure 1. The miR396/GRF Balance Regulates Root Meristem Size and Growth.

In the micrographs, the white arrowheads mark the position of the QC, the yellow arrowheads mark the end of the meristem (Mz) where cells start to elongate, and the green arrowheads mark the end of the elongation zone (Ez).

(A) Depiction of a typical *GRF* gene. Note the miR396 target site (black box) and the interaction of *GRFs* with a mutant version of miR396 (miR396_7-8insG), which has a higher interaction energy. Also note the insertion of an additional nucleotide (highlighted in red) in miR396_7-8insG that eliminates the bulge present in the interaction between miR396 and the *GRFs*.

To determine the relevance of the repression by miR396 of specific *GRFs*, we analyzed the effect of silent mutations on the miR396 target site of *GRF2* and *GRF3*. These mutations abolish the interaction with the miRNA, creating miRNA-resistant *GRFs* (*rGRF2* and *rGRF3*) (Figure 2A). These *GRF* transgenes are transcribed from their own promoter regions but are insensitive to posttranscriptional repression by miR396. Both *rGRF2* and *rGRF3* plants accumulated higher levels of the corresponding *GRF* (Supplemental Figure 5A) and had defects in root growth (Supplemental Figures 5B and 5C). Analysis at the cellular level revealed a reduction in meristem size by *rGRF2* and *rGRF3* (Figures 2C and 2D) without any obvious effect on cell elongation (Supplemental Figures 5D and 5E).

To confirm that the downregulation of the *GRFs* was responsible for the meristem size increase of *35S:miR396* plants, we generated a dexamethasone (DEX)-inducible allele of *rGRF3* expressed from its own promoter (*rGRF3-GR*). We introduced this construct into Arabidopsis plants and crossed them with plants harboring *35S:miR396*. As expected, the resulting *35S:miR396* × *rGRF3-GR* plants have an enlarged meristem with respect to wild-type plants (Figure 2E). Treatment of *35S:miR396* × *rGRF3-GR* plants with DEX rescued the long-meristem phenotype (Figure

(B) and **(C)** Expression of GFP reporters of *GRF2* **(B)** and *GRF3* **(C)**. *GRF* reporters are C-terminal translational fusions of *GFP* to the complete gene, including introns and their own promoter sequences. Bars = 50 µm.

(D) Root tip architecture 7 d after sowing of wild-type and *grf1 grf2 grf3* triple mutant plants. Bar = 50 µm.

(E) Root growth phenotype 7 d after sowing of wild-type plants and three independent transgenic plants (*35S:miR396*) overexpressing increasing levels of miR396. Numerals above the photographs indicate the miR396 levels relative to wild-type roots as estimated by RT-qPCR. Bar = 1 cm.

(F) Root tip architecture in wild-type plants and plants from two representative transgenic lines expressing increasing amounts of miR396 (*35S:miR396* #1 and #2, which accumulate 90- or 4-fold more miR396 compared with the wild type, respectively). Bar = 50 µm.

(G) Root tip architecture in plants from transgenic lines overexpressing miR396_7-8insG. This miRNA is an artificial miRNA created using the *MIR319A* precursor backbone. Bar = 50 µm.

(H) Number of cortex cells in the root meristem (Nm) of wild-type (Ws accession) and *grf1 grf2 grf3* triple mutant plants. The asterisk indicates a significant difference from wild-type roots as determined by Student's *t* test ($P < 0.05$). Ten cortex cell files from 10 plants of each genotype were scored for the number of meristematic cortex cells. The data shown are means ± SE of 10 biological replicates.

(I) Number of cortex cells in the root meristem of wild-type (Col-0) and *35S:miR396 #2* plants. The asterisk indicates a significant difference from the wild type as determined by Student's *t* test ($P < 0.05$). Ten cortex cell files from 10 plants of each genotype were scored for the number of meristematic cortex cells. The data shown are means ± SE of 10 biological replicates.

(J) Length of cortex cells in the root meristem of wild-type (Col-0) and *35S:miR396 #2* plants. The asterisk indicates a significant difference from the wild type as determined by Student's *t* test ($P < 0.05$). At least 10 meristematic cortex cells from 10 plants were measured. The data shown are means ± SE of 100 individual cells.

(K) Length of mature cortex cells of wild-type (Col-0) and *35S:miR396 #2* plants. At least 10 mature cortex cells from 10 plants were measured. The data shown are means ± SE of 100 individual cells.

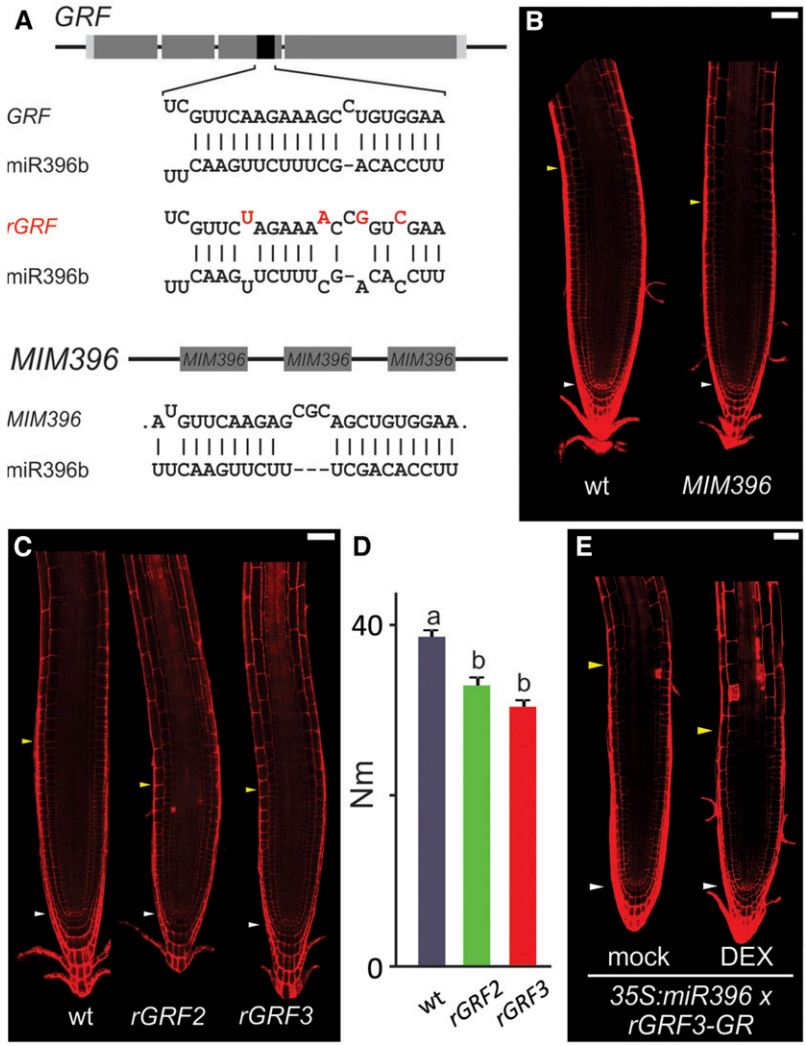

Figure 2. Disruption of miR396 Activity Reduces the Root Meristem Size.

(A) Strategies to inactivate miR396 activity. Top, a typical *GRF* gene showing the miR396 (*GRF*) and the miR396-resistant (*rGRF*) target sites paired with miR396b. Synonymous mutations that alter the interaction with miR396 are shown in red. Bottom, the miR396 target mimic (*MIM396*) paired with miR396b.
(B) Inactivation of miR396 in *MIM396* reduces the size of the root meristem. Bar = 50 µm.
(C) Root tip architecture 7 d after sowing in wild-type, *rGRF2*, and *rGRF3* plants. The white arrowheads mark the position of the QC, while the yellow arrowheads mark the end of the meristem where cells start to elongate. Bar = 50 µm.
(D) Number of cortex cells in the root meristem (Nm) of wild-type (Col-0), *rGRF2*, and *rGRF3* plants. Different letters indicate significant differences as determined by ANOVA followed by Tukey's multiple comparison test ($P < 0.05$). Ten cortex cell files from 10 plants were scored for the number of meristematic cortex cells. The data shown are means ± SE of 10 biological replicates.
(E) Complementation of the long-meristem phenotype of *35S:miR396* plants by a DEX-inducible *rGRF3* (*rGRF3-GR*) after DEX treatment (5 µM, 72 h). Bar = 50 µm.

2E), confirming the importance of the miR396:GRF ratio in the control of root meristem size.

miR396 Modulates Cycling Cells

Despite their enlarged meristems, *35S:miR396* plants displayed a short-root phenotype, which might seem a contradiction at first sight. We hypothesized that the reduced levels of the *GRFs* were affecting the properties of the TACs. As a well-known characteristic of the TACs is a rapid division rate, we decided to analyze the duration of their cell cycle. An estimation of the average cell cycle duration of meristematic cortex cells (Ivanov and Dubrovsky, 1997) indicated an increase in *35S:miR396* and a reduction in *rGRF3* when compared with wild-type cells (Figure 3A).

We then used an experimental assay based on whole root cell cycle synchronization (Cools et al., 2010) to study the properties of the cell cycle in *35S:miR396* and *rGRF3* plants. We measured the transcript levels of the mitotic *CYCLINB1;2* and *CYCLIN*

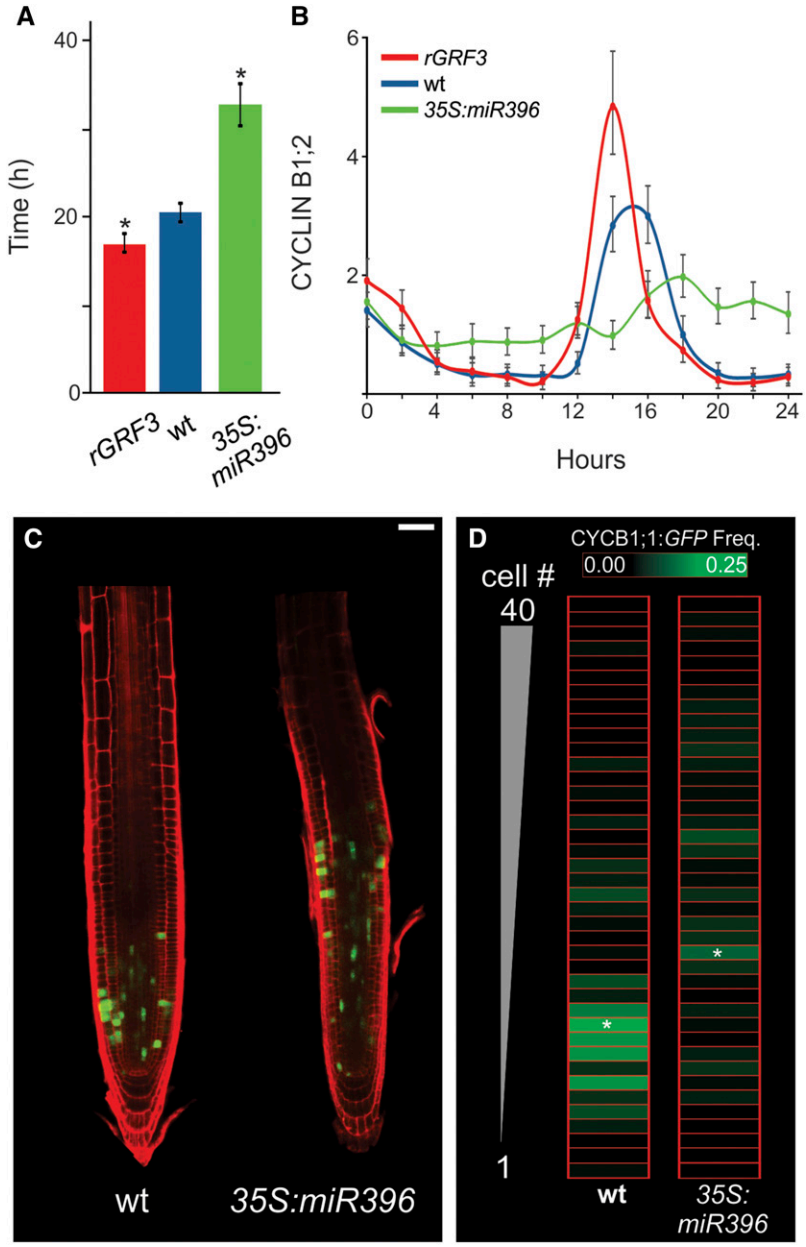

Figure 3. Control of Cycling Cells by miR396.

(A) Average duration of the cell division cycle in meristematic cortex cells in wild-type (blue), *rGRF3* (red), and *35S:miR396* (green) roots. Asterisks indicate significant differences from the wild type as determined by Student's *t* test ($P < 0.05$). The data shown are means ± SE of 10 biological replicates.
(B) Time-course expression analysis of a mitotic marker (*CYCLINB1;2*) in cell cycle-synchronized root tips from wild-type, *rGRF3*, and *35S:miR396* plants as estimated by RT-qPCR. The data shown are means ± SE of three biological replicates.
(C) Shootward displacement of dividing cells in *35S:miR396* root apical meristems as revealed by a *CYCB1;1:GFP* reporter. Bar = 50 μm.
(D) Heat map showing the frequency of *CYCB1;1:GFP*-positive cells at a given distance from the QC quantified by the number of cortical cells. Note the shootward shift of the maximum frequencies (asterisks). The distribution of *CYCB1;1:GFP*-expressing cells was scored from the cell adjacent to the QC (1) up to cell 40. Thirty-six cortex cell files from 18 plants for each genotype were scored.

DEPENDENT KINASE B2;1 in the synchronized roots. Expression of these markers appeared earlier in *rGRF3* with respect to wild-type roots (Figure 3B; Supplemental Figure 6). By contrast, the peak levels of these markers were both delayed and reduced in a *35S:miR396* background with respect to wild-type roots (Figure 3B; Supplemental Figure 6). Therefore, we propose that the *GRFs* not only affect the timely expression of mitotic cell cycle markers but also contribute to increasing their levels.

These results indicate that the balance between miR396 and *GRFs* regulates the duration of the cell cycle in TACs, explaining

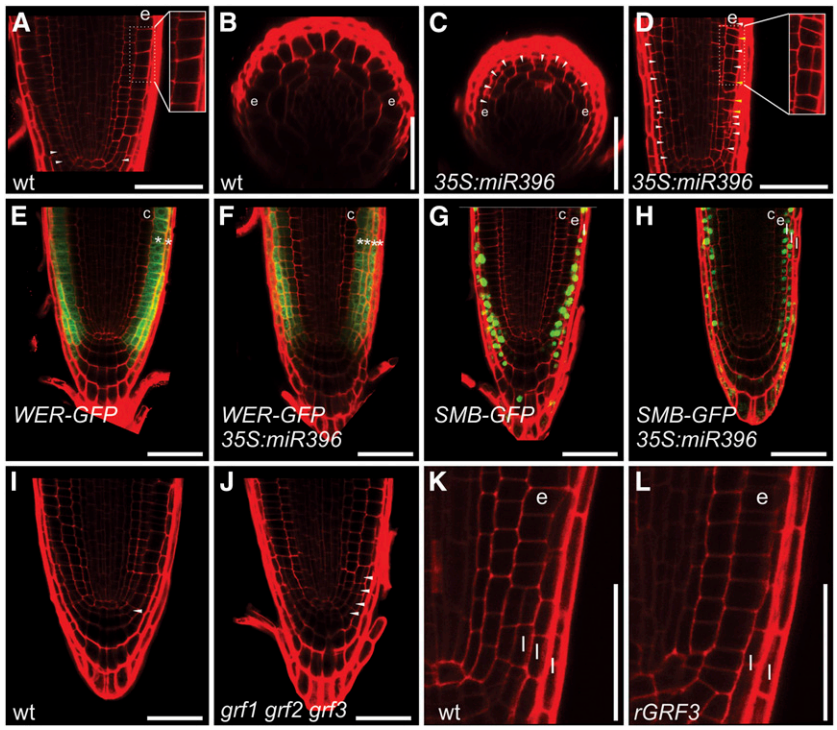

Figure 4. Modified Pattern of Periclinal Cell Divisions in Plants with Changes in the miR396/GRF System.

(A) to **(D)** *35S:miR396* stimulates periclinal cell divisions. White arrowheads mark periclinal cell divisions, and yellow arrowheads mark amplifying anticlinal cell divisions. **(A)** and **(D)** show longitudinal sections of wild-type **(A)** (Col-0) and *35S:miR396* **(D)** roots. **(B)** and **(C)** show cross sections of wild-type **(B)** (Col-0) and *35S:miR396* **(C)** roots 100 μm above the QC, where no periclinal cell divisions occurs in the Ep (e) of wild-type plants. Bars = 50 μm.
(E) and **(F)** *WER-GFP* accumulation in wild-type **(E)** and *35S:miR396* **(F)** roots. c indicates the cortex cell layer, and asterisks indicate Ep and LRC layers. Bars = 50 μm.
(G) and **(H)** Expression of LRC-specific marker (*SMB-GFP*) expression in wild-type **(G)** and *35S:miR396* **(H)** roots. l indicates LRC cells. Bars = 50 μm.
(I) and **(J)** Periclinal cell divisions in the Ep/LRC initials in wild-type (Ws) **(I)** and *grf1 grf2 grf3* **(J)** mutant plants. White arrowheads mark periclinal cell divisions. Bars = 50 μm.
(K) and **(L)** Reduced number of LRC layers in *rGRF3* **(L)** compared with wild-type **(K)** plants. Bars = 50 μm.

the overall reduction of root growth in *35S:miR396* plants despite their enlarged meristems (Figure 1F and 1G). Furthermore, a delayed cell cycle probably explains the increase in cell size observed in the meristems of *35S:miR396* plants (Figure 1J).

Furthermore, expression of the G2-M-specific *CYCLINB1;1* reporter within the TAC zone was located farther from the QC in *35S:miR396* as compared with wild-type roots (Figures 3C and 3D), indicating that the miR396/GRF node affects functions in addition to the speed of the cell cycle, which might also be related to the establishment of the developmental zones along the longitudinal axis of the root.

miR396 Controls Periclinal Cell Divisions

Periclinal cell divisions of the stem cells can generate asymmetric daughters that produce different cell types, such as the epidermis (Ep)/lateral root cap (LRC) initials that generate the Ep and LRC cell layers. Once generated, these cells switch to anticlinal cell divisions, amplifying each of the cell types in the meristem before differentiation occurs (Campilho et al., 2006; Rost, 2011).

Typically, one or two cells are observed in wild-type plants with periclinal cell divisions, generating the Ep and LRC layers (Figures 4A and 4B; Supplemental Figure 7) (Campilho et al., 2006). Compared with the wild type, *35S:miR396* plants harbored a significantly increased number of periclinal divisions that extended throughout the meristem (Figures 4C and 4D; Supplemental Figure 7A). As expected, an increase in the periclinal divisions occurred in *grf1 grf2 grf3* mutants as well (Figures 4I and 4J; Supplemental Figure 7C).

The LRC/Ep marker *WER-GFP* confirmed a higher number of cell layers external to the cortex cells in *35S:miR396* plants (Figures 4E and 4F). *SOMBRERO* (*SMB*), a root cap-specific NAC domain transcription factor, is expressed just after the asymmetric cell division that generates the root cap cells. It has been shown to prevent further generative divisions and promote cell maturation (Willemsen et al., 2008; Bennett et al., 2010; Fendrych et al., 2014). The analysis of an *SMB-GFP* reporter in *35S:miR396* plants confirmed that the extra periclinal cell divisions generated extra LRC cells outside the Ep cell layer (Figures 4G and 4H), supporting a higher stem cell character of the distal portion of the meristem in these plants. Most of the ectopic periclinal divisions detected in *35S:miR396* plants were associated

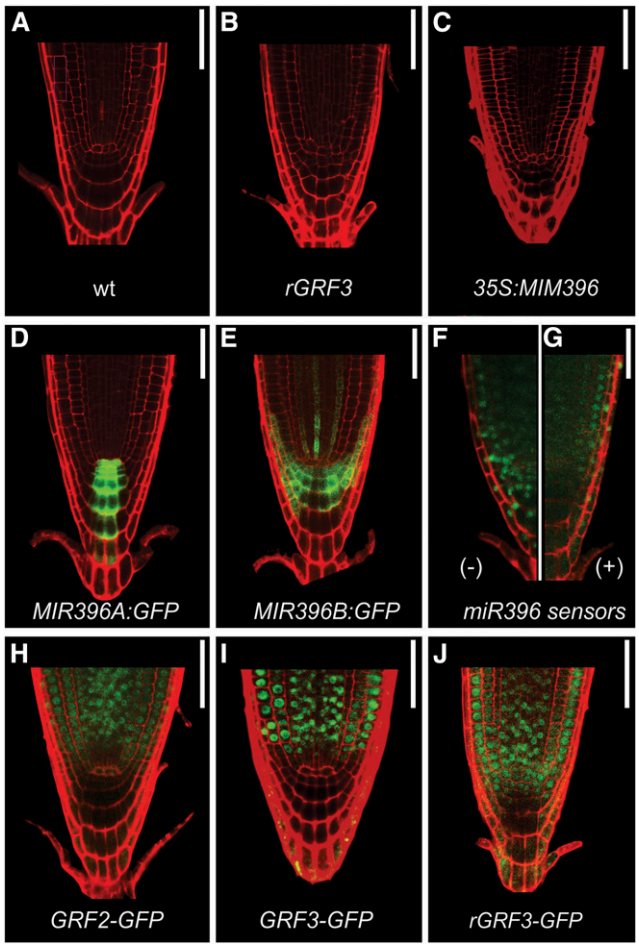

Figure 5. Posttranscriptional Repression of the *GRFs* by miR396 in the SCN.

(A) to **(C)** SCN defects in *rGRF3* **(B)** and *MIM396* **(C)** in comparison with wild-type **(A)** plants. Bars = 50 μm.
(D) and **(E)** Expression patterns of *MIR396A* **(D)** and *MIR396B* **(E)** transcriptional GFP reporters. Bars = 50 μm.
(F) and **(G)** Region of miR396 activity detected with a sensor consisting of a nucleus-localized GFP without **(F)** (−) or with a miR396 binding site **(G)** (+). Bar = 50 μm.
(H) to **(J)** Expression pattern of *GRF2* **(H)**, *GRF3* **(I)**, and miR396-resistant *GRF3* (*rGRF3*) **(J)** translational GFP reporters. Bars = 50 μm.

with the LRC/Ep cell layers; however, RT-qPCR experiments also showed an increase of *CYCD6;1* levels in *35S:miR396* roots (Supplemental Figure 7D), which is necessary for the asymmetric cell division that generates cortex and endodermal cells (Sozzani et al., 2010; Cruz-Ramírez et al., 2012).

On the other hand, plants expressing *rGRF3* and *rGRF2* had a reduced number of LRC layers (Figures 4K and 4L; Supplemental Figure 8) and a low number of periclinal divisions associated with the Ep/LRC initials (Supplemental Figures 7A and 8). Accordingly, *MIM396* plants also had fewer periclinal divisions (Supplemental Figure 7B), resembling the effect of *rGRF3*. Taken together, these results further support the importance of the miR396/GRF network in regulating the transition between stem cells and transit-amplifying cells.

miR396 Excludes the GRFs from the SCN

Further analysis of the stem cell region of *rGRF3* plants revealed a distorted QC and columella cells displaying abnormal cell division patterns (Figure 5B). *MIM396* plants also had a distorted QC (Figure 5C). Thus, repression of *GRFs* by miR396 is necessary for the homeostasis and function of the SCN. Consistent with this hypothesis, we found that *MIR396a* was strongly expressed in the QC and the columella (Figure 5D; Supplemental Figure 9A). We detected *MIR396b* at lower levels, which is consistent with small RNA sequencing data indicating that miR396a is the most abundant isoform in roots (Breakfield et al., 2012; Jeong et al., 2013). Still, we detected the expression of *MIR396b* in the

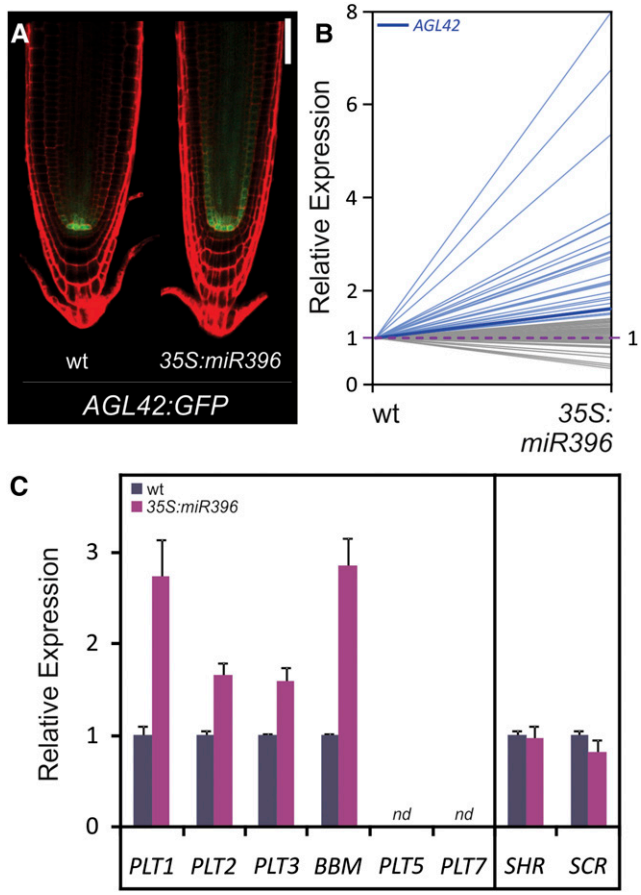

Figure 6. Expanded Expression of SCN Markers in *35S:miR396* Plants.

(A) Expression of a GFP reporter specific for QC and adjacent stele and ground tissue stem cells (*AGL42:GFP*) in wild-type and *35S:miR396* root tips. Bar = 50 μm.
(B) Relative expression of genes coexpressed with *AGL42* in the root meristems of wild-type and *35S:miR396* plants. The light blue lines represent genes whose expression increases significantly in *35S:miR396* root meristems (21 out of 88 genes). The dark blue line highlights the expression of *AGL42*. The purple dotted line indicates values equal to 1.
(C) *PLT*, *SHR*, and *SCR* expression in microdissected root apical meristems from *35S:miR396* roots as estimated with ATH1 microarrays. *nd*, not detected. The data shown are means ± SE of three biological replicates.

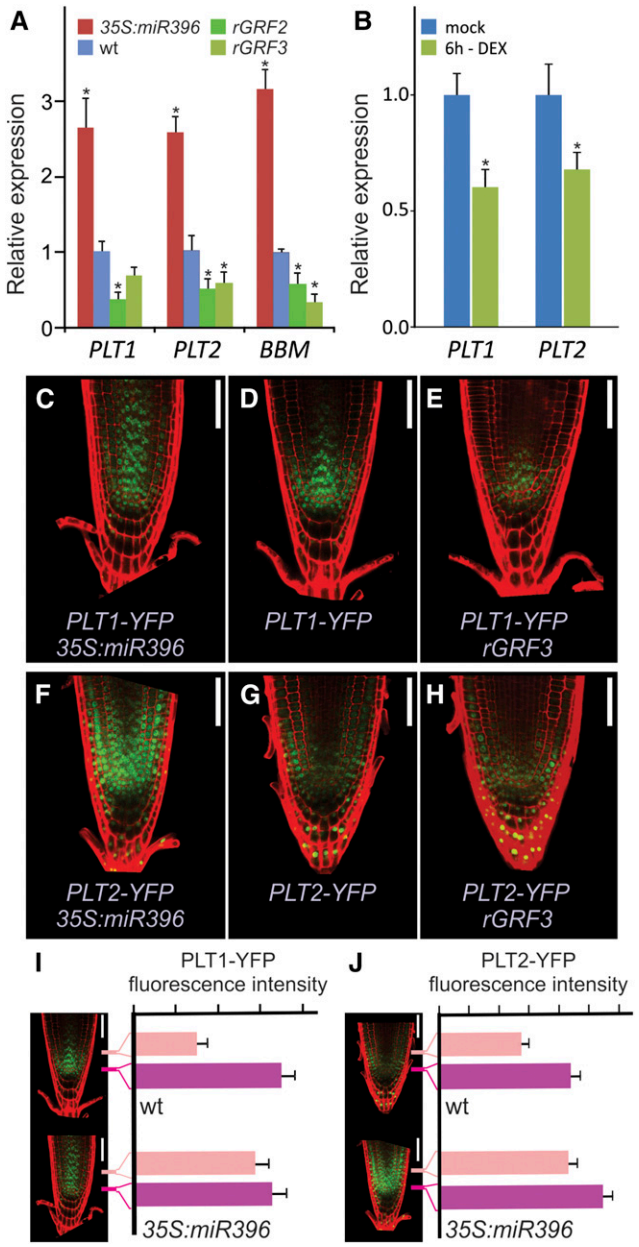

Figure 7. The miR396/GRF Regulatory Module Regulates the Gradient Distribution of *PLT* Genes.

(A) Expression of *PLT1*, *PLT2*, and *BBM* in *35S:miR396* and *rGRF* root tips as estimated by RT-qPCR. The data shown are means ± SE of three biological replicates. Asterisks indicate significant differences from the wild type as determined by Student's *t* test ($P < 0.05$).

(B) Expression of *PLT1* and *PLT2* after treatment with DEX (10 μM, 6 h) of plants transformed with an inducible *rGRF3* (*rGRF3-GR*). The data shown are means ± SE of three biological replicates. Asterisks indicate significant differences from the wild type as determined by Student's *t* test ($P < 0.05$).

(C) to **(H)** Modified gradients of PLT1 and PLT2 in *35S:miR396* and *rGRF3* roots. Bars = 50 μm.

(I) and **(J)** Quantification of the fluorescence intensity of proteins produced by *PLT1-YFP* **(I)** and *PLT2-YFP* **(J)** reporters in wild-type and *35S:miR396* root meristems. Purple bars indicate the QC region, while pink bars represent a region in the stele 50 μm above. The data shown are means ± SE of eight biological replicates. Bars = 50 μm.

columella, the Ep/LRC initials, and the LRC and, at lower levels, in the meristematic zone (Figure 5E; Supplemental Figure 9B).

The activity of miR396 in the SCN was confirmed using a miR396 sensor (Figures 5F and 5G; Supplemental Figure 10). Furthermore, although the wild-type *GRF3-GFP* reporter was absent in the SCN (Figure 5I), a miR396-insensitive *GRF3-GFP* reporter (*rGRF3-GFP*) expanded its expression toward the SCN (Figure 5J). In particular, *GRF3-GFP* was absent in the LRC/Ep stem cell initials and was only present in cells undergoing anticlinal amplifying divisions (Figure 5I), whereas *rGRF3-GFP* had an expanded expression pattern, invading the presumptive SCN area (Figure 5J). A similar result was obtained with *GRF2* (Figure 5H; Supplemental Figure 11), demonstrating that the activity of miR396 excludes *GRF* transcription factors from the stem cells.

Downregulation of the GRFs Activates the Expression of Stem Cell Markers in TACs

AGAMOUS-LIKE42 (*AGL42*) is a MADS box transcription factor whose expression is enriched in the QC and adjacent stele and ground tissue stem cells (Nawy et al., 2005) (*AGL42:GFP*; Figure 6A). Overexpression of miR396 caused *AGL42:GFP* to be expressed in a broader area, consistent with a shootward expansion of the SCN in plants having reduced *GRF* levels (Figure 6A).

To define the networks regulated by the miR396/GRF regulatory node, we performed transcriptome profiling of microdissected meristems of wild-type versus *35S:miR396* roots and discovered 600 induced and 135 repressed genes ($P < 0.01$ and fold change > 50%; Supplemental Table 1). Interestingly, a substantial number of genes that are coexpressed with *AGL42* (Brady et al., 2007) were upregulated in the *35S:miR396* root samples (Figure 6B; Supplemental Table 2).

Next, we analyzed this data set for changes in the expression of genes important for the establishment of the SCN. While there was no change in the expression of *SCR* or *SHR*, several *PLT* genes were upregulated in the *35S:miR396* transcript profiling data set (Figure 6C). Transcript levels for *PLT1*, *PLT2*, and *BBM* were increased in *35S:miR396* plants (Figure 7A; Supplemental Figure 12) but downregulated in plants expressing *rGRF2* or *rGRF3* (Figure 7A). Also, *rGRF3-GR* plants treated with DEX for 6 h showed a downregulation of *PLT1* and *PLT2* (Figure 7B).

PLT proteins have an expression maximum in the stem cell area, and their distribution forms a gradient along the longitudinal axis of the root (Figures 7D and 7G; Supplemental Figure 13A). This is instrumental for their function as dose-dependent regulators of root development (Galinha et al., 2007; Mähönen et al., 2014). The expression maxima of both PLT1-YFP and PLT2-YFP were reduced in the stem cell area by *rGRF3*, and their gradients faded away more abruptly compared with wild-type plants (Figures 7E and 7H; Supplemental Figures 13B and 13C). By contrast, both *PLT* genes were expressed at high levels in a broader region of *35S:miR396* roots (Figures 7C, 7F, 7I, and 7J; Supplemental Figure 13A).

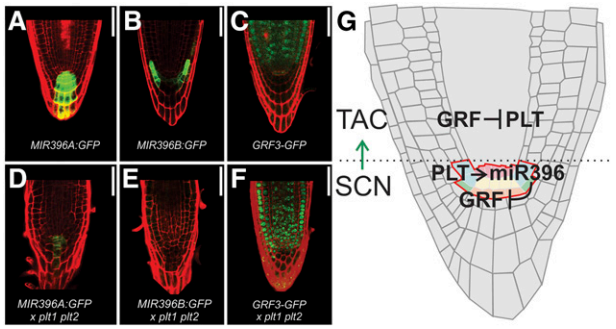

Figure 8. PLT Activity Is Necessary for *MIR396* Expression in the SCN.

(A) to **(F)** Expression of *MIR396A:GFP* (**[A]** and **[D]**), *MIR396B:GFP* (**[B]** and **[E]**), and *GRF3-GFP* (**[C]** and **[F]**) reporters in wild-type (**[A]** to **[C]**) and *plt1 plt2* mutant (**[D]** to **[F]**) plants. Bars = 50 µm.

(G) Proposed model by which the regulatory interactions between miR396, *GRF*, and *PLT* define the transition between stem cells and transit-amplifying cells.

As high *PLT1* and *PLT2* levels are associated with stem cell identity, the extended expression maxima are consistent with a potential expanded stem cell-like character in root meristems of *35S:miR396* (Figures 3C and 3D, 4, and 6A and 6B). Taken together, our results indicate that the miR396-regulated *GRFs* act as *PLT* repressors, controlling their expression pattern and abundance along the longitudinal axis of the root.

PLT Genes Are Necessary for the Expression of *MIR396* Genes in the SCN

Because high PLT levels are necessary for the proper activity of the SCN (Aida et al., 2004; Galinha et al., 2007; Mähönen et al., 2014) and miR396 excludes *GRFs* from the same area (Figure 5), we reasoned that PLT itself might be required for the expression of *MIR396* genes in the SCN. Indeed, we found that the expression of both *MIR396* genes was significantly reduced in *plt1 plt2* (Figure 8; Supplemental Figure 14). Consistent with these findings, although *GRF3* expression is excluded from the SCN in wild-type roots, its expression extended into the SCN region in the *plt1 plt2* double mutant (Figures 8C and 8F). Finally, *PLT2-YFP* plants, which accumulate increased levels of PLT2 compared with wild-type plants, have an enlarged meristem (Mähönen et al., 2000), have more periclinal divisions in the Ep cell layer, and accumulate higher levels of mature miR396 (Supplemental Figure 15). These results indicate that the high *PLT* levels present in the SCN are necessary for the activation of *MIR396* genes, which in turn excludes the *GRFs* from the stem cells.

DISCUSSION

GRFs Are Markers of Transit-Amplifying Cells in Roots

The expression of both *GRF2* and *GRF3* was detected specifically in TACs. Neither *GRF2* nor *GRF3* was detected in the columella stem cells or in their daughters, the columella cells. As this tissue does not go through a transit-amplifying phase (Petricka et al., 2012), *GRF* expression seems to occur only in cells that undergo mitotic cycles to amplify the number of already established cell types.

GRF genes have regulatory sequences that are able to drive their transcription in a broader region, most conspicuously in the root SCN. This was shown through the introduction of mutations that prevent the binding of miR396 to *GRF2* or *GRF3* or by inactivating miR396 through target mimicry. Therefore, post-transcriptional repression by miR396 is essential to achieve the normal tissue-specific expression pattern of the *GRFs*.

In leaves, miR396 is highly expressed in expanding and differentiating cells and generates a basipetal gradient of expression of the *GRFs*, which coincides with proliferating cells (Rodriguez et al., 2010; Debernardi et al., 2012). Therefore, modifying *GRF* expression by miR396 seems to be a recurrent strategy to ensure that specific cells express these transcription factors. Interestingly, while *MIR396b* is the most highly expressed member of the miR396 family in leaves (Debernardi et al., 2012; Jeong et al., 2013; Liang et al., 2014a; Schommer et al., 2014), *MIR396a* is the most highly expressed in roots (Breakfield et al., 2012; Jeong et al., 2013; this work). *MIR396b* is induced in leaves by TCP4 (Schommer et al., 2014), a transcription factor involved in the repression of cell proliferation and the promotion of cell differentiation (Efroni et al., 2008; Schommer et al., 2014). In roots, we observed that *MIR396* expression depends on *PLT* genes, indicating that miR396 is recurrently activated during development by different regulators.

GRFs Repress Stem Cell-Like Properties in TACs

The transition between stem cells and TACs in the Arabidopsis root is sharp, and the daughters of the stem cells immediately enter a defined pathway characterized by anticlinal cell divisions that amplify the established cell types. A decrease in *GRF* levels blurred this sharp transition: periclinal cell divisions, which are typical of stem cells, were observed among TACs, whereas markers of the QC and the stem cells extended their expression into the meristem. Cells in the SCN also proliferate at a much slower frequency than the surrounding transit-amplifying meristematic cells (Dolan et al., 1993; Kerk et al., 2000; Campilho et al., 2006; Cruz-Ramírez et al., 2013; Heyman et al., 2013), and a modification of the *GRF* levels in TACs modified the cell cycle length accordingly.

In addition, the peak of transit-amplifying cell divisions was shifted away from the stem cells, as has been reported recently for plants expressing high levels of *PLT* (Mähönen et al., 2014). Two pathways, directed by PLT and the SHR/SCR transcription factors, establish the QC and the stem cells (Petricka et al., 2012; Heyman et al., 2014). That only *PLT* transcripts responded to miR396 levels suggests that the GRFs specifically repress genes that establish stem cells.

It was recently shown that high auxin levels produce a narrow domain of *PLT* transcription from which PLT protein further spreads through growth dilution and cell-to-cell movement, generating a gradient of expression with a maxima in the SCN (Mähönen et al., 2014). In addition to these processes, our results show that downregulation of PLT levels in TACs is an active process that requires the activity of the GRFs. We propose that GRFs contribute to shape the gradient that defines the root

developmental zones. In this way, reduction in GRF activity causes a shootward expansion of the PLT gradient. The GRFs affected PLT transcript and protein levels. Because PLT protein is stabilized by secreted peptides (Matsuzaki et al., 2010; Zhou et al., 2010), we cannot rule out that the GRFs have an additional effect on the protein stability.

PLT1 has been shown to be repressed in the apical part of the embryo by *HANABA TARANU* and *ANGUSTIFOLIA3* (*AN3*) (Kanei et al., 2012). AN3 has been also shown to interact with GRF transcription factors (Kim and Kende, 2004; Horiguchi et al., 2005; Debernardi et al., 2014), so we cannot dismiss the notion that the GRFs repress PLT genes in other tissues as well. However, our data show that the repression of *PLT* genes by the GRFs contributes to the quantitative regulation of PLT levels in the root meristem, as a reduction in the *GRFs* by miR396 or an increase in their levels by the use of *rGRF* transgenes or miR396 target mimics results in opposite changes of PLT expression levels. It is interesting that, in the most extreme cases, miR396 overexpression produces defects in cell elongation, which were also observed previously (Bao et al., 2014). Cell elongation is also inhibited by high local levels of PLT (Mähönen et al., 2014). Therefore, we propose that the interplay between miR396, the GRFs, and PLT transcription factors can also affect cell elongation in the most extreme cases.

The expansion of stem cell-like properties of the root meristem in plants with high levels of miR396 likely explains the decrease in the rate of the cell cycle and the increase of root meristem size. Therefore, we think that miR396 fulfills different functions in roots or the aerial part of the plant. Although we observed that miR396 is highly expressed in root stem cells and that its ectopic expression expands the domain of cells with stem cell-like properties, in leaves miR396 is associated with differentiating cells and its ectopic expression induces differentiation of the proliferating cells (Rodriguez et al., 2010; Debernardi et al., 2012). Still, in both tissues, the *GRF* transcription factors are expressed in rapidly dividing cells, which is ensured at least partially by the activity of miR396.

miR396-Mediated Exclusion of GRFs Is Essential for SCN Function

Reporters for both *MIR396A* and *MIR396B* promoters showed their highest expression in the SCN and columella cells. This activity of miR396 in the SCN was further validated by the use of a miR396 sensor and *GRF* reporter constructs. Each *MIRNA* was expressed in a specific subset of cells, suggesting that different signals contribute to their regulation, although the expression of both *MIRNAs* requires PLT activity.

Transgenes expressing miR396-resistant versions of *GRF2* or *GRF3* resulted in the expression of GRF transcription factors in the SCN, distorted QC, and columella cells. These results are consistent with a positive role of the GRFs in the promotion of the cell cycle. Roots with defects in miR396 activity, caused by the expression of either a miR396 target mimic or a miR396-resistant *GRF*, showed defects in the activity of the Ep/LRC initials, which is opposite to that seen in *grf1 grf2 grf3* mutants or *35S:miR396*. Exclusion of the *GRFs* seems to be necessary for periclinal cell divisions to occur, as can be seen in TACs with low *GRF* levels. A similar effect can be achieved by increasing PLT levels (Galinha et al., 2007). In turn, defects in the activity of the Ep/LRC initials and shorter meristems, as seen in *rGRF3*-expressing plants, are similar to the phenotypes observed in knockouts of PLT genes (Aida et al., 2004), further indicating that these transcription factors have opposite functions in the specification of stem cells and TACs.

The miR396/*GRF* network has been implicated in the developmental reprogramming processes unleashed upon biotic interactions of roots with cyst nematodes (Hewezi et al., 2012) or symbiotic rhizobia (Subramanian et al., 2008; Bazin et al., 2013). It would be interesting to determine if the mutual repression between *GRFs* and *PLT* described here also operates in the development of the specialized organs settled in each case.

The Regulatory Interaction between miR396, GRF, and PLT Controls the Transition of Stem Cells to Transit-Amplifying Cells

Taken together, our results indicate that the interactions between miR396, *GRFs*, and *PLTs* are required for the transition of stem cells into transit-amplifying cells. In the SCN, PLTs activate miR396, which excludes the *GRFs*. The *GRFs* become active in the transit-amplifying cells and dampen PLT expression (Figure 8G). In this way, miR396 establishes a molecular boundary to exclude GRFs from the SCN and set up a sharp transition from slowly proliferating cells with the capacity to generate different cell types to cells that amplify rapidly in number to ensure appropriate organ growth.

METHODS

Plant Materials, Growth Conditions, and Treatments

Arabidopsis thaliana accession Col-0 was used in most of the experiments. See Supplemental Table 4 for a list and a description of the transgenic lines and mutants used in this study. The miRNA target motif in *GRFs* was altered by introducing synonymous mutations into a wild-type *GRF* genomic fragment using the QuikChange Site Directed Mutagenesis Kit (Stratagene).

Arabidopsis mutants *plt1 plt2* (Galinha et al., 2007) and *grf1 grf2 grf3* (Kim et al., 2003) are in the Wassilewskija (Ws) accession. The transgenic marker lines *PLT1-YFP*, *PLT2-YFP* (Galinha et al., 2007), *WER-GFP* (Lee and Schiefelbein, 1999), *AGL42:GFP* (Nawy et al., 2005), and *SMB-GFP* (Fendrych et al., 2014) have been described previously.

Plants were grown in long photoperiods (16 h of light/8 h of dark) at 100 μmol photons m^{-2} s^{-1} at 21°C. For root analysis, plants were grown vertically on 1× Murashige and Skoog salt mixture, 1% sucrose, and 2.3 mM MES, pH 5.8, in 1% agar. DEX (Sigma-Aldrich) was stored as 10 mM stocks in ethanol and used at the indicated concentrations (5 to 10 μM) for the indicated periods (6 to 72 h). The root meristem was synchronized in the G1/S transition using hydroxyurea as described (Cools et al., 2010), and the expression of cell cycle markers was followed by RT-qPCR.

Expression Analysis

Total RNA was isolated from root tissue using Tripure isolation reagent (Roche). Total RNA (0.5 μg) was treated with RQ1 RNase-free DNase (Promega). Then, first-strand cDNA synthesis was performed using SuperScript III Reverse Transcriptase (Invitrogen). PCR was performed in a Mastercycler ep realplex thermal cycler (Eppendorf) using SYBR Green I

(Roche) to monitor double-stranded DNA synthesis. qPCR for each gene was done on at least three biological replicates with technical duplicates for each biological replicate. The relative transcript level was determined for each sample, normalized to the *PROTEIN PHOSPHATASE2A* cDNA level (Czechowski et al., 2005). Mature miR396 levels were determined by stem-loop RT-qPCR as described previously (Debernardi et al., 2012). Primer sequences are given in Supplemental Table 3. To visualize GUS reporter activity, roots of transgenic plants were subjected to GUS staining, as described previously (Donnelly et al., 1999).

Microarray Analyses

Total RNA was extracted using the mirVana miRNA Isolation Kit (Ambion) from microdissected meristems of wild-type and *35S:miR396* roots grown on vertical square plates ($10 \times 10 \times 2$ cm) for 7 d. Microarray analyses using the Affymetrix ATH1 platform were performed on three biological replicates as described (Schmid et al., 2005). Normalized expression estimates were obtained using Guanine-Cytosine Robust Multi-Array Average (GCRMA) (http://www.bioconductor.org) (Irizarry et al., 2003), and significant changes were calculated by using logit-T (Lemon et al., 2003).

Microscopy

Roots were stained with 10 μg/mL propidium iodide for 1 min and mounted in water. Laser confocal scanning microscopy was performed with a 20×, 0.75-NA lens on a Nikon Eclipse TE-2000-E microscope equipped with a C1-si confocal scanning head, using the 488-nm laser line for excitation, a 515/30-nm band-pass filter for GFP and YFP detection, and a 605/75-nm band-pass filter for propidium iodide detection. Cellular parameters and fluorescence signal intensity were analyzed with Fiji (Schindelin et al., 2012). The average length of meristematic cortex cells was estimated by determining the average cell size from the 5th to the 15th cell from the QC. The average duration of the cell cycle (T) for meristematic cortex cells was calculated for each individual root using the following equation: $T = (\ln 2\ Nm\ Le)\ V^{-1}$, where Nm is the number of meristematic cells in one file of the cortex, Le is the length of fully elongated cortex cells in μm, and V is the root growth rate calculated as μm/h (Ivanov and Dubrovsky, 1997).

Accession Numbers

Accession numbers (Arabidopsis Genome Initiative locus identifiers) for the genes described here are provided in Supplemental Table 3. Microarray data have been deposited in the Gene Expression Omnibus database (GSE58807).

Supplemental Data

Supplemental Figure 1. *GRFs* in Root Development.

Supplemental Figure 2. Molecular and Cellular Characterization of *35S:miR396* #2.

Supplemental Figure 3. Overexpression of a Hyperactive miR396 Variant Causes Stronger Root Phenotypes.

Supplemental Figure 4. Decreased Meristem Size in *MIM396* Plants.

Supplemental Figure 5. Characterization of *rGRF2* and *rGRF3* Plants.

Supplemental Figure 6. Control of Cycling Cells by miR396.

Supplemental Figure 7. Number of Periclinal Cell Divisions in Ep/LRC Initials of *35S:miR396*, *rGRF3*, *MIM396*, and *grf1 grf2 grf3* Plants.

Supplemental Figure 8. *rGRF2* Perturbs the Stem Cell Niche and Modifies the Pattern of Periclinal Divisions.

Supplemental Figure 9. Expression Pattern of *MIR396* Genes.

Supplemental Figure 10. A miR396 Sensor Is Excluded from the Stem Cell Niche.

Supplemental Figure 11. Posttranscriptional Regulation of *GRF2* by miR396.

Supplemental Figure 12. Quantitative Regulation of PLT by the miR396/*GRF* Network.

Supplemental Figure 13. Regulation of PLT Expression Gradient by the miR396/*GRF* Network.

Supplemental Figure 14. PLT Activity Is Necessary for MIR396 Expression in the SCN.

Supplemental Figure 15. PLT Induces miR396 to Exclude GRFs from the SCN.

Supplemental Table 1. Genes Differentially Expressed in *35S:miR396* Root Meristems as Compared with the Wild Type.

Supplemental Table 2. Expression of *AGL42* Coexpressed Genes in *35S:miR396* Root Meristems as Compared with the Wild Type.

Supplemental Table 3. Locus IDs and Oligonucleotide Primers Used in RT-qPCR.

Supplemental Table 4. Binary Plasmids Used in This Study to Generate Transgenic Lines.

ACKNOWLEDGMENTS

We thank Ben Scheres for the *plt1 plt2* mutants and the PLT1:*PLT1-YFP* and PLT2:*PLT2-YFP* reporters; Jen Hoe Kim for the *grf1 grf2 grf3* mutant; Moritz Nowack for the *SMB-GFP* reporter; Alexis Maizel, Renze Heidstra, Ben Scheres, and members of the Benfey and Palatnik laboratory for advice and reading of the article; and Rodrigo Vena, Enrique Morales, and Lia Pietrasanta for help with microscope imaging. M.F.E., J.M.D., and M.A.M. were supported by fellowships from CONICET. M.F.E. was also supported by the Josefina Prats Foundation. T.C. is a Postdoctoral Fellow of the Research Foundation-Flanders. R.E.R. and J.F.P. are members of CONICET. P.N.B.'s laboratory was supported by the National Institutes of Health (Grant R01-GM043778) and by the Gordon and Betty Moore Foundation (through Grant GBMF3405). R.E.R. was supported by ANPCyT (Grants PICT2010/1847 and PICT2012/1686). The majority of studies were supported by grants to J.F.P. (ANPCyT and Howard Hughes Medical Institute).

AUTHOR CONTRIBUTIONS

R.E.R. and J.F.P. designed the research. R.E.R., M.F.E., J.M.D., N.W.B., M.A.M., M.S., and T.C. performed research. R.E.R., M.F.E., T.C., L.D.V., and J.F.P. analyzed data. R.E.R., L.D.V., P.N.B., and J.F.P. contributed reagents and materials. R.E.R. and J.F.P. wrote the article.

Received May 22, 2015; revised September 30, 2015; accepted November 11, 2015; published December 8, 2015.

REFERENCES

Aida, M., Beis, D., Heidstra, R., Willemsen, V., Blilou, I., Galinha, C., Nussaume, L., Noh, Y.S., Amasino, R., and Scheres, B. (2004). The PLETHORA genes mediate patterning of the Arabidopsis root stem cell niche. Cell **119:** 109–120.

Bao, M., Bian, H., Zha, Y., Li, F., Sun, Y., Bai, B., Chen, Z., Wang, J., Zhu, M., and Han, N. (2014). miR396a-mediated basic helix-loop-helix transcription factor bHLH74 repression acts as a regulator for root growth in Arabidopsis seedlings. Plant Cell Physiol. **55:** 1343–1353.

Bazin, J., Khan, G.A., Combier, J.P., Bustos-Sanmamed, P., Debernardi, J.M., Rodriguez, R., Sorin, C., Palatnik, J., Hartmann, C., Crespi, M., and Lelandais-Brière, C. (2013). miR396 affects mycorrhization and root meristem activity in the legume *Medicago truncatula*. Plant J. **74:** 920–934.

Bennett, T., van den Toorn, A., Sanchez-Perez, G.F., Campilho, A., Willemsen, V., Snel, B., and Scheres, B. (2010). SOMBRERO, BEARSKIN1, and BEARSKIN2 regulate root cap maturation in Arabidopsis. Plant Cell **22:** 640–654.

Bologna, N.G., and Voinnet, O. (2014). The diversity, biogenesis, and activities of endogenous silencing small RNAs in Arabidopsis. Annu. Rev. Plant Biol. **65:** 473–503.

Brady, S.M., Orlando, D.A., Lee, J.Y., Wang, J.Y., Koch, J., Dinneny, J.R., Mace, D., Ohler, U., and Benfey, P.N. (2007). A high-resolution root spatiotemporal map reveals dominant expression patterns. Science **318:** 801–806.

Breakfield, N.W., Corcoran, D.L., Petricka, J.J., Shen, J., Sae-Seaw, J., Rubio-Somoza, I., Weigel, D., Ohler, U., and Benfey, P.N. (2012). High-resolution experimental and computational profiling of tissue-specific known and novel miRNAs in Arabidopsis. Genome Res. **22:** 163–176.

Campilho, A., Garcia, B., Toorn, H.V., Wijk, H.V., Campilho, A., and Scheres, B. (2006). Time-lapse analysis of stem-cell divisions in the Arabidopsis thaliana root meristem. Plant J. **48:** 619–627.

Cools, T., Iantcheva, A., Maes, S., Van den Daele, H., and De Veylder, L. (2010). A replication stress-induced synchronization method for *Arabidopsis thaliana* root meristems. Plant J. **64:** 705–714.

Cruz-Ramírez, A., et al. (2012). A bistable circuit involving SCARECROW-RETINOBLASTOMA integrates cues to inform asymmetric stem cell division. Cell **150:** 1002–1015.

Cruz-Ramírez, A., Díaz-Triviño, S., Wachsman, G., Du, Y., Arteága-Vázquez, M., Zhang, H., Benjamins, R., Blilou, I., Neef, A.B., Chandler, V., and Scheres, B. (2013). A SCARECROW-RETINOBLASTOMA protein network controls protective quiescence in the Arabidopsis root stem cell organizer. PLoS Biol. **11:** e1001724. **Czechowski, T., Stitt, M., Altmann, T., Udvardi, M.K., and Scheible, W.R.** (2005). Genome-wide identification and testing of superior reference genes for transcript normalization in Arabidopsis. Plant Physiol. **139:** 5–17.

Debernardi, J.M., Mecchia, M.A., Vercruyssen, L., Smaczniak, C., Kaufmann, K., Inze, D., Rodriguez, R.E., and Palatnik, J.F. (2014). Post-transcriptional control of GRF transcription factors by microRNA miR396 and GIF co-activator affects leaf size and longevity. Plant J. **79:** 413–426.

Debernardi, J.M., Rodriguez, R.E., Mecchia, M.A., and Palatnik, J.F. (2012). Functional specialization of the plant miR396 regulatory network through distinct microRNA-target interactions. PLoS Genet. **8:** e1002419.

Dolan, L., Janmaat, K., Willemsen, V., Linstead, P., Poethig, S., Roberts, K., and Scheres, B. (1993). Cellular organisation of the *Arabidopsis thaliana* root. Development **119:** 71–84.

Donnelly, P.M., Bonetta, D., Tsukaya, H., Dengler, R.E., and Dengler, N.G. (1999). Cell cycling and cell enlargement in developing leaves of Arabidopsis. Dev. Biol. **215:** 407–419.

Efroni, I., Blum, E., Goldshmidt, A., and Eshed, Y. (2008). A protracted and dynamic maturation schedule underlies Arabidopsis leaf development. Plant Cell **20:** 2293–2306.

Fendrych, M., Van Hautegem, T., Van Durme, M., Olvera-Carrillo, Y., Huysmans, M., Karimi, M., Lippens, S., Guerin, C.J., Krebs, M., Schumacher, K., and Nowack, M.K. (2014). Programmed cell death controlled by ANAC033/SOMBRERO determines root cap organ size in Arabidopsis. Curr. Biol. **24:** 931–940.

Franco-Zorrilla, J.M., Valli, A., Todesco, M., Mateos, I., Puga, M.I., Rubio-Somoza, I., Leyva, A., Weigel, D., García, J.A., and Paz-Ares, J. (2007). Target mimicry provides a new mechanism for regulation of microRNA activity. Nat. Genet. **39:** 1033–1037.

Galinha, C., Hofhuis, H., Luijten, M., Willemsen, V., Blilou, I., Heidstra, R., and Scheres, B. (2007). PLETHORA proteins as dose-dependent master regulators of Arabidopsis root development. Nature **449:** 1053–1057.

Heidstra, R., and Sabatini, S. (2014). Plant and animal stem cells: similar yet different. Nat. Rev. Mol. Cell Biol. **15:** 301–312.

Hewezi, T., Maier, T.R., Nettleton, D., and Baum, T.J. (2012). The Arabidopsis microRNA396-GRF1/GRF3 regulatory module acts as a developmental regulator in the reprogramming of root cells during cyst nematode infection. Plant Physiol. **159:** 321–335.

Heyman, J., Cools, T., Vandenbussche, F., Heyndrickx, K.S., Van Leene, J., Vercauteren, I., Vanderauwera, S., Vandepoele, K., De Jaeger, G., Van Der Straeten, D., and De Veylder, L. (2013). ERF115 controls root quiescent center cell division and stem cell replenishment. Science **342:** 860–863.

Heyman, J., Kumpf, R.P., and De Veylder, L. (2014). A quiescent path to plant longevity. Trends Cell Biol. **24:** 443–448.

Horiguchi, G., Kim, G.T., and Tsukaya, H. (2005). The transcription factor AtGRF5 and the transcription coactivator AN3 regulate cell proliferation in leaf primordia of *Arabidopsis thaliana*. Plant J. **43:** 68–78.

Irizarry, R.A., Ooi, S.L., Wu, Z., and Boeke, J.D. (2003). Use of mixture models in a microarray-based screening procedure for detecting differentially represented yeast mutants. Stat Appl Genet Mol Biol **2:** Article 1.

Ivanov, V.B., and Dubrovsky, J.G. (1997). Estimation of the cell-cycle duration in the root apical meristem: A model of linkage between cell-cycle duration, rate of cell production, and rate of root growth. Int. J. Plant Sci. **158:** 757–763.

Jeong, D.H., Thatcher, S.R., Brown, R.S., Zhai, J., Park, S., Rymarquis, L.A., Meyers, B.C., and Green, P.J. (2013). Comprehensive investigation of microRNAs enhanced by analysis of sequence variants, expression patterns, ARGONAUTE loading, and target cleavage. Plant Physiol. **162:** 1225–1245.

Jones-Rhoades, M.W., and Bartel, D.P. (2004). Computational identification of plant microRNAs and their targets, including a stress-induced miRNA. Mol. Cell **14:** 787–799.

Kanei, M., Horiguchi, G., and Tsukaya, H. (2012). Stable establishment of cotyledon identity during embryogenesis in Arabidopsis by ANGUSTIFOLIA3 and HANABA TARANU. Development **139:** 2436–2446.

Kerk, N.M., Jiang, K., and Feldman, L.J. (2000). Auxin metabolism in the root apical meristem. Plant Physiol. **122:** 925–932.

Kim, J., and Lee, B. (2006). GROWTH-REGULATING FACTOR4 of *Arabidopsis thaliana* is required for development of leaves, cotyledons, and shoot apical meristem. J. Plant Biol. **49:** 463–468.

Kim, J.H., Choi, D., and Kende, H. (2003). The AtGRF family of putative transcription factors is involved in leaf and cotyledon growth in Arabidopsis. Plant J. **36:** 94–104.

Kim, J.H., and Kende, H. (2004). A transcriptional coactivator, AtGIF1, is involved in regulating leaf growth and morphology in Arabidopsis. Proc. Natl. Acad. Sci. USA **101:** 13374–13379.

Koster, M.I., and Roop, D.R. (2007). Mechanisms regulating epithelial stratification. Annu. Rev. Cell Dev. Biol. **23:** 93–113.

Lee, M.M., and Schiefelbein, J. (1999). WEREWOLF, a MYB-related protein in Arabidopsis, is a position-dependent regulator of epidermal cell patterning. Cell **99:** 473–483.

Lemon, W.J., Liyanarachchi, S., and You, M. (2003). A high performance test of differential gene expression for oligonucleotide arrays. Genome Biol. **4:** R67.

Levesque, M.P., Vernoux, T., Busch, W., Cui, H., Wang, J.Y., Blilou, I., Hassan, H., Nakajima, K., Matsumoto, N., Lohmann, J.U., Scheres, B., and Benfey, P.N. (2006). Whole-genome analysis of the SHORT-ROOT developmental pathway in Arabidopsis. PLoS Biol. **4:** e143.

Liang, C., Liu, X., Sun, Y., Yiu, S.M., and Lim, B.L. (2014a). Global small RNA analysis in fast-growing *Arabidopsis thaliana* with elevated concentrations of ATP and sugars. BMC Genomics **15:** 116.

Liang, G., He, H., Li, Y., Wang, F., and Yu, D. (2014b). Molecular mechanism of microRNA396 mediating pistil development in Arabidopsis. Plant Physiol. **164:** 249–258.

Liu, D., Song, Y., Chen, Z., and Yu, D. (2009). Ectopic expression of miR396 suppresses GRF target gene expression and alters leaf growth in Arabidopsis. Physiol. Plant. **136:** 223–236.

Lui, J.H., Hansen, D.V., and Kriegstein, A.R. (2011). Development and evolution of the human neocortex. Cell **146:** 18–36.

Mähönen, A.P., Bonke, M., Kauppinen, L., Riikonen, M., Benfey, P.N., and Helariutta, Y. (2000). A novel two-component hybrid molecule regulates vascular morphogenesis of the Arabidopsis root. Genes Dev. **14:** 2938–2943.

Mähönen, A.P., ten Tusscher, K., Siligato, R., Smetana, O., Díaz-Triviño, S., Salojärvi, J., Wachsman, G., Prasad, K., Heidstra, R., and Scheres, B. (2014). PLETHORA gradient formation mechanism separates auxin responses. Nature **515:** 125–129.

Mallory, A.C., Elmayan, T., and Vaucheret, H. (2008). MicroRNA maturation and action: The expanding roles of ARGONAUTEs. Curr. Opin. Plant Biol. **11:** 560–566.

Matsuzaki, Y., Ogawa-Ohnishi, M., Mori, A., and Matsubayashi, Y. (2010). Secreted peptide signals required for maintenance of root stem cell niche in Arabidopsis. Science **329:** 1065–1067.

Nakajima, K., Sena, G., Nawy, T., and Benfey, P.N. (2001). Intercellular movement of the putative transcription factor SHR in root patterning. Nature **413:** 307–311.

Nawy, T., Lee, J.Y., Colinas, J., Wang, J.Y., Thongrod, S.C., Malamy, J.E., Birnbaum, K., and Benfey, P.N. (2005). Transcriptional profile of the Arabidopsis root quiescent center. Plant Cell **17:** 1908–1925.

Petricka, J.J., Winter, C.M., and Benfey, P.N. (2012). Control of Arabidopsis root development. Annu. Rev. Plant Biol. **63:** 563–590.

Pysh, L.D., Wysocka-Diller, J.W., Camilleri, C., Bouchez, D., and Benfey, P.N. (1999). The GRAS gene family in Arabidopsis: sequence characterization and basic expression analysis of the SCARECROW-LIKE genes. Plant J. **18:** 111–119.

Rodriguez, R.E., Mecchia, M.A., Debernardi, J.M., Schommer, C., Weigel, D., and Palatnik, J.F. (2010). Control of cell proliferation in *Arabidopsis thaliana* by microRNA miR396. Development **137:** 103–112.

Rost, T.L. (2011). The organization of roots of dicotyledonous plants and the positions of control points. Ann. Bot. (Lond.) **107:** 1213–1222.

Sabatini, S., Heidstra, R., Wildwater, M., and Scheres, B. (2003). SCARECROW is involved in positioning the stem cell niche in the Arabidopsis root meristem. Genes Dev. **17:** 354–358.

Sarkar, A.K., Luijten, M., Miyashima, S., Lenhard, M., Hashimoto, T., Nakajima, K., Scheres, B., Heidstra, R., and Laux, T. (2007). Conserved factors regulate signalling in *Arabidopsis thaliana* shoot and root stem cell organizers. Nature **446:** 811–814.

Scheres, B. (2007). Stem-cell niches: nursery rhymes across kingdoms. Nat. Rev. Mol. Cell Biol. **8:** 345–354.

Schindelin, J., et al. (2012). Fiji: An open-source platform for biological-image analysis. Nat. Methods **9:** 676–682.

Schmid, M., Davison, T.S., Henz, S.R., Pape, U.J., Demar, M., Vingron, M., Schölkopf, B., Weigel, D., and Lohmann, J.U. (2005). A gene expression map of *Arabidopsis thaliana* development. Nat. Genet. **37:** 501–506.

Schommer, C., Debernardi, J.M., Bresso, E.G., Rodriguez, R.E., and Palatnik, J.F. (2014). Repression of cell proliferation by miR319-regulated TCP4. Mol. Plant **7:** 1533–1544.

Sozzani, R., Cui, H., Moreno-Risueno, M.A., Busch, W., Van Norman, J.M., Vernoux, T., Brady, S.M., Dewitte, W., Murray, J.A., and Benfey, P.N. (2010). Spatiotemporal regulation of cell-cycle genes by SHORTROOT links patterning and growth. Nature **466:** 128–132.

Subramanian, S., Fu, Y., Sunkar, R., Barbazuk, W.B., Zhu, J.K., and Yu, O. (2008). Novel and nodulation-regulated microRNAs in soybean roots. BMC Genomics **9:** 160.

Todesco, M., Rubio-Somoza, I., Paz-Ares, J., and Weigel, D. (2010). A collection of target mimics for comprehensive analysis of microRNA function in *Arabidopsis thaliana*. PLoS Genet. **6:** e1001031.

Willemsen, V., Bauch, M., Bennett, T., Campilho, A., Wolkenfelt, H., Xu, J., Haseloff, J., and Scheres, B. (2008). The NAC domain transcription factors FEZ and SOMBRERO control the orientation of cell division plane in Arabidopsis root stem cells. Dev. Cell **15:** 913–922.

Zhou, W., Wei, L., Xu, J., Zhai, Q., Jiang, H., Chen, R., Chen, Q., Sun, J., Chu, J., Zhu, L., Liu, C.M., and Li, C. (2010). Arabidopsis Tyrosylprotein sulfotransferase acts in the auxin/PLETHORA pathway in regulating postembryonic maintenance of the root stem cell niche. Plant Cell **22:** 3692–3709.